Cellular and Molecular Life Sciences (2021) 78:2145–2155
https://doi.org/10.1007/s00018-020-03623-7

ORIGINAL ARTICLE

The pro-apoptotic domain of BIM protein forms toxic amyloid fibrils

Ravit Malishev[1] · Shani Ben-Zichri[1] · Ofek Oren[3] · Nitzan Shauloff[1] · Tal Peretz[2] · Ran Taube[3] · Niv Papo[4] · Raz Jelinek[1]

Received: 21 February 2020 / Revised: 26 June 2020 / Accepted: 14 August 2020 / Published online: 25 August 2020

Abstract

BIM is a key apoptotic protein, participating in diverse cellular processes. Interestingly, recent studies have hypothesized that BIM is associated with the extensive neuronal cell death encountered in protein misfolding diseases, such as Alzheimer's disease. Here, we report that the core pro-apoptotic domain of BIM, the BIM-BH3 motif, forms ubiquitous amyloid fibrils. The BIM-BH3 fibrils exhibit cytotoxicity, disrupt mitochondrial functions, and modulate the structures and dynamics of mitochondrial membrane mimics. Interestingly, a slightly longer peptide in which BIM-BH3 was flanked by four additional residues, widely employed as a model of the pro-apoptotic core domain of BIM, did not form fibrils, nor exhibited cell disruptive properties. The experimental data suggest a new mechanistic role for the BIM-BH3 domain, and demonstrate, for the first time, that an apoptotic peptide forms toxic amyloid fibrils.

Keywords Bcl-2 proteins · BIM · Mitochondria · Apoptosis · Fibrils · Beta-amyloid

Introduction

Apoptosis, a fundamental physiological process of programmed cell death, is critical for development and functions of multicellular organisms [1]. Apoptosis is regulated by a number of specialized proteins, primary among those are the B cell lymphoma-2 (Bcl-2) regulatory protein family which are mostly localized in the mitochondria [2]. Bcl-2 proteins share the distinct Bcl-2 homology (BH) domains which are pivotal is homodimer and heterodimer formation among different Bcl-2 proteins [3]. Scheme 1 depicts the BH3 motif, shared by several pro-apoptotic Bcl-2 proteins, which has a prominent role in triggering apoptosis through docking onto hydrophobic clefts in the Bcl-2 targets [4, 5].

The Bcl-2-interacting mediator of cell death (BIM) protein, which also contains the BH3 domain (Scheme 1), is expressed by cells of hematopoietic, neuronal, and epithelial lineage, and it is essential for homeostasis [5]. BIM exhibits high affinity to almost all anti-apoptotic Bcl-2 proteins [6], in addition directly activates pro-apoptotic effectors, such as BAX [7]. Numerous investigations have focused on deciphering the structural and functional features underlining BIM activity, primarily the contribution of the BIM-BH3 domain (encircled in Scheme 1). The BH3-only proteins are intrinsically unstructured [8]; however, several studies have shown that the BH3 domain adopted amphipathic α-helices upon binding to hydrophobic grooves on the surfaces of target Bcl-2 proteins [9]. Significant research efforts have been directed towards mapping the core BIM-BH3 sequence responsible for protein binding and triggering pro-apoptotic processes [10].

Importantly, while the roles of BIM in apoptosis is well established, this protein has been also recently associated with protein misfolding diseases such as Alzheimer's disease (AD) [11], Parkinson's disease [12], and Huntington's

Electronic supplementary material The online version of this article (https://doi.org/10.1007/s00018-020-03623-7) contains supplementary material, which is available to authorized users.

✉ Raz Jelinek
razj@bgu.ac.il

[1] Department of Chemistry and Ilse, Katz Institute for Nanotechnology, Ben Gurion University of the Negev, 84105 Beer Sheva, Israel

[2] Department of Life Sciences, Ben-Gurion University of the Negev, 84105 Beer Sheva, Israel

[3] The Shraga Segal Department of Microbiology, Immunology and Genetics, Faculty of Health Sciences, Ben-Gurion University of the Negev, 84105 Beer Sheva, Israel

[4] Avram and Stella Goldstein-Goren Department of Biotechnology Engineering and the National Institute of Biotechnology in the Negev, Ben-Gurion University of the Negev, 84105 Beer Sheva, Israel

disease [13]. For example, there have been studies indicating elevated levels of BIM in AD-afflicted neuronal cells [14–16]. Protein misfolding diseases are characterized by aggregation of distinctive amyloidogenic proteins such as beta-amyloid in AD [17], amylin (type II diabetes, [18]), and huntingtin (Huntington's disease, [19]). Intriguingly, it is becoming increasingly evident that diverse proteins and peptides adopt amyloid fibril organizations, and that such fibrillar species exert varied physiological effects, both adversarial to cells and tissues, but also functionally-important [20, 21].

Here, we demonstrate that the core BIM-BH3 domain adopts a β-sheet conformation and undergoes rapid, extensive fibrillation. The BIM-BH3 fibrils exhibited cell toxicity, and exerted significant disruption of mitochondrial functionalities and membrane integrity. Notably, a slightly longer peptide comprising BIM-BH3 flanked by four additional residues, which has been often employed in previous studies as a BIM-BH3 model, did not produce fibrils nor exhibited cell disruptive properties. The experimental data we present demonstrate, for the first time, that BIM-BH3, a prominent pro-apoptotic domain, forms amyloid fibrils, and that the BIM-BH3 fibrils are toxic and disrupt mitochondrial functions. Interestingly, we also discovered that BIM-BH3 and Aβ, when mixed, form a pronounced amyloid fibril network, more extensive than either peptide individually. Overall, this work may point to yet unrecognized pathological roles for BIM-BH3 which could be related to its fibrillation propensity. This study may also shed new light on putative links between apoptotic proteins and the pathological facets of amyloid diseases.

Results and discussion

The striking observation reported here is the formation of ubiquitous BIM-BH3 fibrils in aqueous solutions. Figure 1 depicts spectroscopic and microscopic characterization of the fibrillation phenomenon. Specifically, the thioflavin-T (ThT) fluorescence assay, widely employed for monitoring β-sheet-containing protein fibrils [22], reveals a direct correlation between ThT fluorescence and BIM-BH3 concentration (Fig. 1a); ThT measurements showed almost instantaneous BIM-BH3 fibril formation upon dissolution of the peptide in buffer (Figure 1, SI). The representative confocal fluorescence microscopy image of ThT-labelled BIM-BH3 in Fig. 1b confirms formation of abundant fibrils in buffer, stained by the ThT dye. The scanning electron microscopy (SEM) image in Fig. 1c further illuminates the network of elongated BIM-BH3 fibrils.

Figure 2 compares the structural properties of BIM-BH3 and the 4-residue extended BIM-BH3 (142–167) peptide domain (Table 1). BIM-BH3 (142–167) has been perceived in many studies as the pro-apoptotic BIM-BH3 peptide model, and utilized for analysis of BIM functionalities and interactions with other apoptotic proteins in the Bcl-2 family

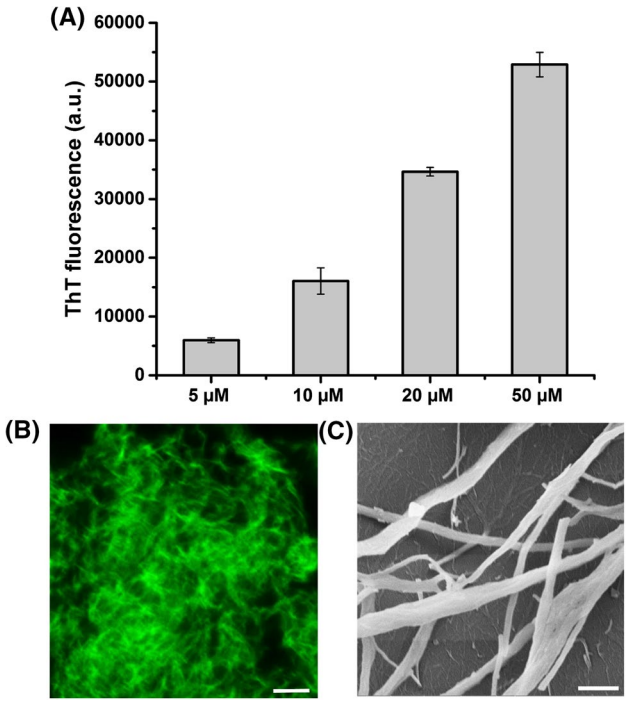

Fig. 1 Fibril formation by BIM-BH3. **a** Thioflavin-T (ThT) fluorescence emission recorded in different BIM-BH3 concentrations. ThT data were acquired after 10-min incubation of the dye with the peptide. **b** Fluorescence microscopy image of Thioflavin-T-stained BIM-BH3 fibrils. Scale bar corresponds to 2 μm. **c** Scanning electron microscopy (SEM) image of 50 μM BIM-BH3. Scale bar corresponds to 500 nm

Scheme 1 The BH3 motif mapped on several pro-apoptotic Bcl-2 proteins. The conserved leucine (L) and aspartate (D) residues are highlighted in yellow. The grey columns correspond to conserved hydrophobic residues

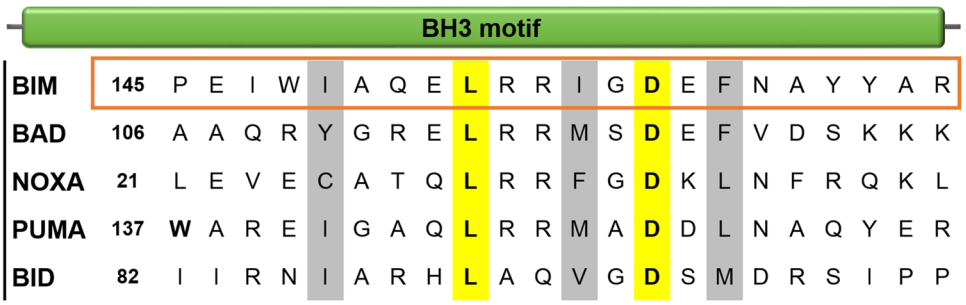

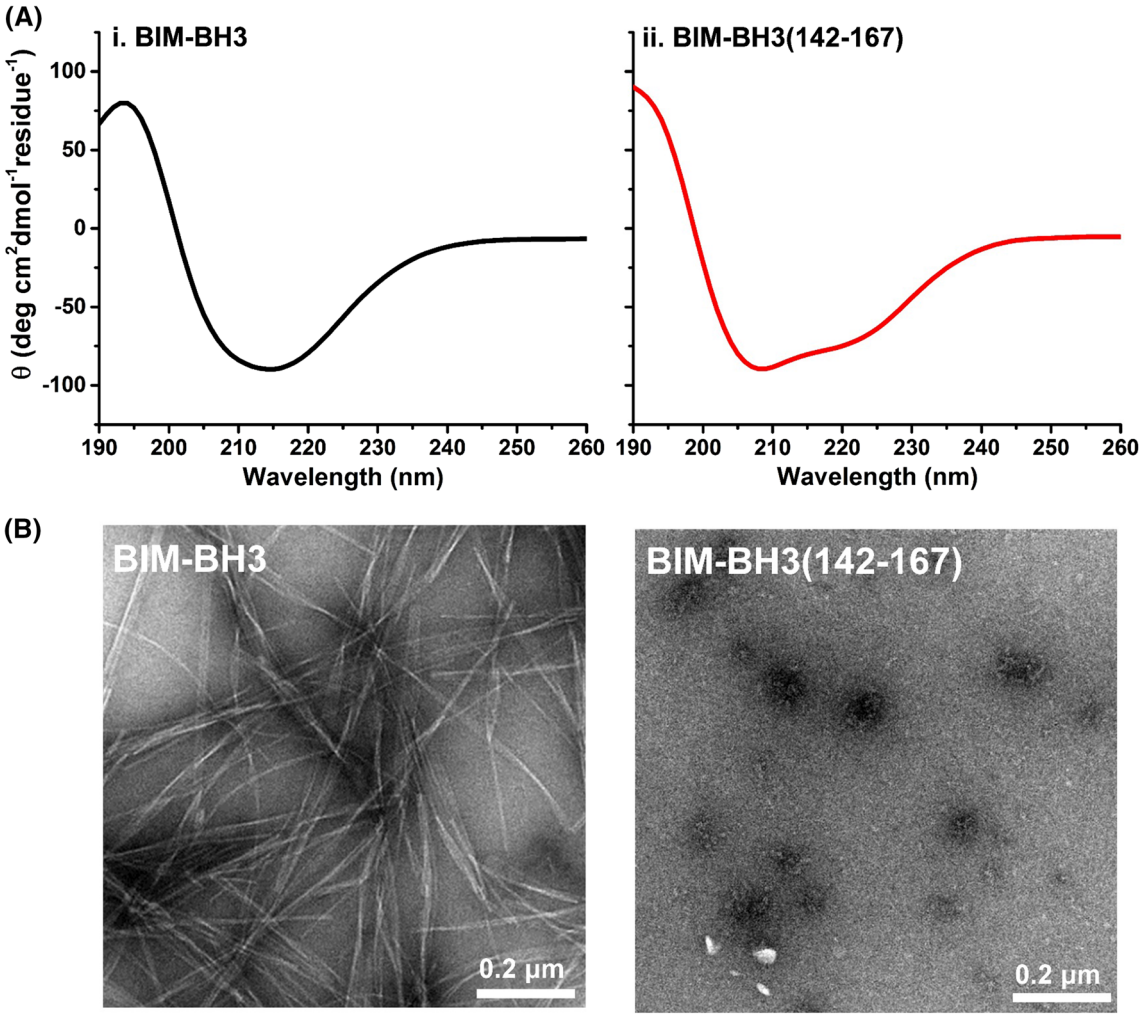

Fig. 2 Secondary structures and fibril morphologies of BIM-BH3 and BIM-BH3 (142–167). **a** Circular dichroism (CD) spectra of (i) BIM-BH3; (ii) BIM-BH3 (142–167) (both 50 µM). **b** Transmission electron microscopy (TEM) of the samples used in the CD experiments

Table 1 Amino acid sequence of the BIM-BH3 motif, and the 25-residue BIM-BH3 (142–167) sequence employed in previous studies focused on the pro-apoptotic domain of BIM [4, 6]

Peptide Name	BH3-motif sequence	Charge
BIM-BH3	PEIWIAQELRRIGDEFNAYYAR	-1
BIM-BH3(142-167)	**DMR**PEIWIAQELRRIGDEFNAYYAR**R**	0

[8, 23]. The circular dichroism (CD) results in Fig. 2a reveal a distinct difference between the secondary structures of the two peptides. Specifically, BIM-BH3 adopted a β-sheet conformation almost instantaneously, reflected in the pronounced negative signal at 218 nm and distinctive peak at 195 nm (Fig. 2a, i). In contrast, BIM-BH3 (142–167) appeared predominantly α-helical, exemplified in the two spectral depressions at 208 nm and 222 nm (Fig. 2a, ii). The pronounced structural difference between the two peptides likely stems from the presence of charged residues in BIM-BH3 (142–167) (aspartic acid and two arginines) and concomitant neutral charge of the peptide [9]. Importantly, CD spectra recorded for the BH3 domains of other Bcl-2 protein family members (e.g., Scheme 1) indicated random secondary structures (Fig. 2, SI), further highlighting the unique fibrillation of BIM-BH3. Furthermore, shorter

peptides comprising the conserved LXXXGDE sequence of BH3 (Scheme 1) also gave rise to random conformations in aqueous solution (Fig. 3, SI), underscoring the unique fibrillation observed in case of the core BIM-BH3 domain.

The transmission electron microscopy (TEM) analysis in Fig. 2b further illuminates the striking differences in aggregation properties between BIM-BH3 and BIM-BH3 (142–167). The TEM images in Fig. 2b, recorded after 30-min incubation, demonstrate extensive fibrillation of BIM-BH3, consistent with the ThT fluorescence and microscopy data in Fig. 1. BIM-BH3 (142–167), on the other hand, did not form fibril morphologies, instead producing small aggregates. The pronounced difference in structural properties and aggregation profiles between the two peptides is significant, due to the fact that BIM-BH3 (142–167) presumably represents, in almost all published reports, the pro-apoptotic domain of BIM [24, 25]. As such, the observation of β-sheet conformation and fibrillation of BIM-BH3, which is the actual pro-apoptotic core domain of BIM, may point to distinct and previously unrecognized physiological activity of this motif.

Fibril formation has been observed in diverse protein systems, and fibrillation phenomena have been linked to several pathological conditions and cytotoxic effects [26, 27]. Accordingly, we carried out experiments designed to assess the cell toxicity profiles of BIM-BH3 and BIM-BH3 (142–167) (Fig. 3). Figure 3a examines the concentration-dependent effects of the two peptides upon SH-SY5Y neuroblastoma cells, often employed as an in vitro model of neuronal functions, using the XTT cell viability assay. The bar diagram in Fig. 3a demonstrates that extracellular BIM-BH3 exhibited significant dose-dependent cytotoxicity. In contrast, the XTT analysis in Fig. 3a indicates that the longer sequence BIM-BH3 (142–167) had only a minor adverse

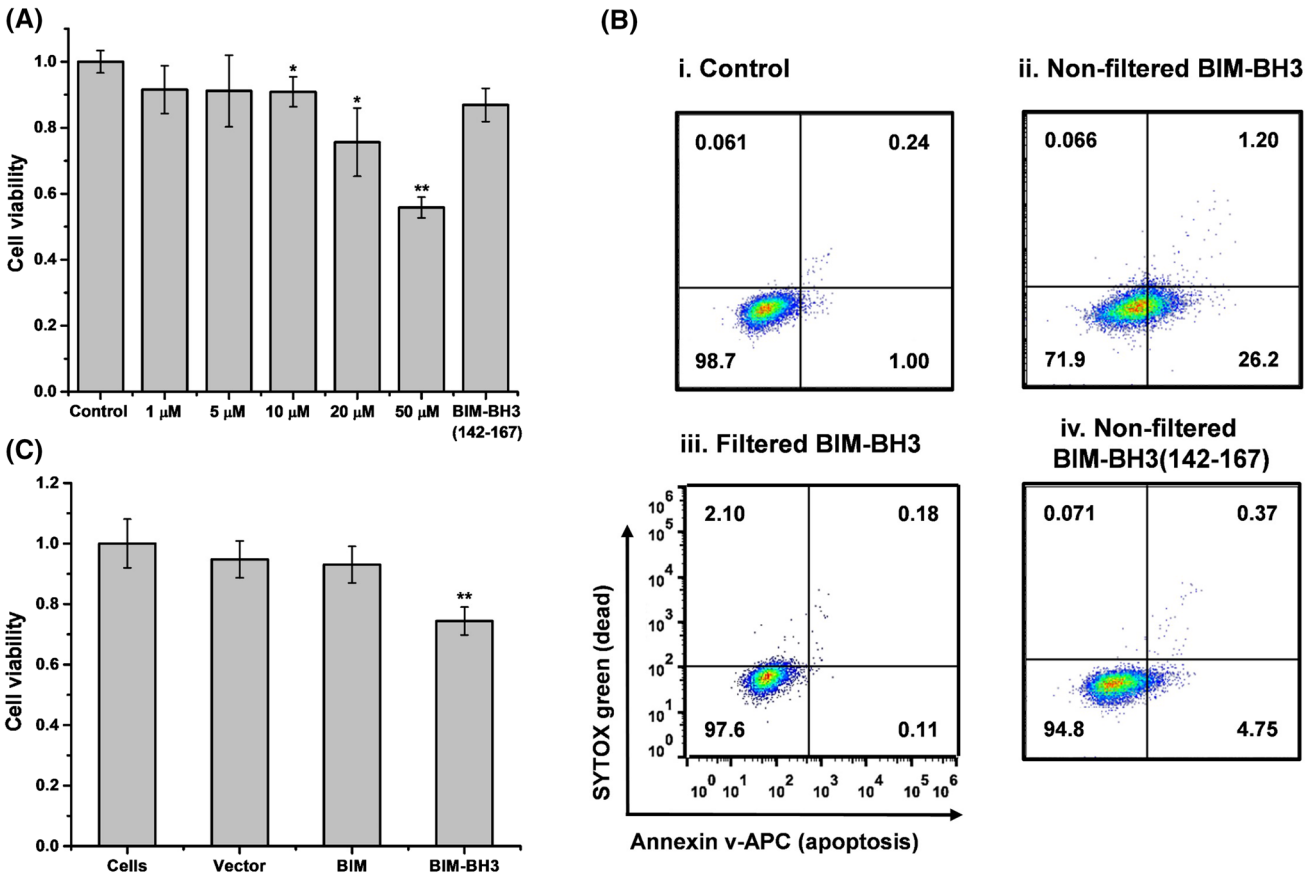

Fig. 3 Cell toxicity of BIM-BH3 fibrils. **a** Cytotoxicity profile of BIM-BH3 determined by the XTT assay. SH-SY5Y cells were incubated with medium containing BIM-BH3 (50 μM) or BIM-BH3 (142–167) (50 μM) for 24 h, followed by addition of the XTT reagent. The control corresponds to SH-SY5Y cells not treated with either peptide. **b** Apoptotic activity monitored by annexin V and SYTOX green staining flow cytometry. (i) Control SH-SY5Y cells (not treated by the peptides); (ii) non-filtered 50 μM BIM-BH3; (iii) filtered 50 μM BIM-BH3; (iv) non-filtered 50 μM BIM-BH3 (142–167). **c** Viability of SH-ST5Y cells, determined by the XTT assay, upon cell transfection with constructs expressing only the cDNA, full length BIM, or BIM-BH3 domain (SH-SY5Y cells transiently expressing either pCMV6-BIM-MYC or pCDNA 3.1-HA-BIM-BH3 as analyzed by confocal microscopy shown in Fig. 4, SI). Results are presented as mean ± standard error of the mean (SEM) of three replicates. *$p < 0.05$ and **$p < 0.001$ are compared to the control of each particular experiment

effect upon cell viability, even at 50 μM, the highest concentration utilized. This result is significant, since both peptides consist of the same core BIM domain; as such, cytotoxicity of BIM-BH3, manifested in Fig. 3a, may be primarily related to the fibrillar organization of the peptide, which is absent in BIM-BH3 (142–167) (e.g., Fig. 2b).

To complement the XTT cell viability assay we performed a fluorescence-activated cell sorting (FACS) experiment using annexin V and SYTOX green staining for apoptosis detection, designed to assess the impact of extracellular BIM-BH3 and BIM-BH3 (142–167) upon cell death processes (utilizing the SH-SY5Y cell model). The experiments were carried out at peptide concentrations of 50 μM, which gave rise to the highest cell mortality by BIM-BH3 according to the XTT cell viability assay (e.g., Fig. 3a). Notably, Fig. 3b reveals that BIM-BH3 induced significant apoptosis, giving rise to 26% apoptotic cell population (Fig. 3b, ii). Crucially, when the BIM-BH3 suspension was passed through a 0.22 μm filter prior to addition to the SH-SY5Y cells—thereby effectively removing the fibrils—no apoptotic effect was apparent (Fig. 3b, iii). This result demonstrates that the primary toxic species in the BIM-BH3 suspension were fibrils, rather than smaller monomeric or oligomeric species, often considered to be the pathogenic factors in amyloidogenic systems [28, 29]. The flow cytometry experiment in Fig. 3b, iv shows that the longer BIM-BH3 (142–167) peptide domain (unfiltered sample) did not induce apoptosis, echoing the XTT cell viability assay result in Fig. 3a and further attesting to the remarkable difference between the physiological impacts of the two peptides.

In addition to toxicity of purified BIM-BH3 fibrils applied extracellularly, we also tested intracellular BIM-BH3-induced toxicity, by comparing the viability of cells expressing BIM-BH3 domain to that of cells expressing the full length BIM, where SH-ST5Y cells expressing only the cDNA served as control (Fig. 3c). Intracellular amyloid fibril accumulation appears to be an early event in varied pathological diseases, and may be a source for extracellular deposits as the disease progresses [30]. Indeed, the XTT assay results in Fig. 3c demonstrate that SH-SY5Y cells expressing BIM-BH3 exhibited significantly lower (~30%) viability compared to cells expressing the empty vector, and even compared to cells expressing the full BIM protein.

To further investigate the effects of BIM-BH3 and BIM-BH3 (142–167) upon fundamental cellular processes, we evaluated the consequences of peptide addition upon mitochondrial functions (Fig. 4). Disruption of mitochondrial functionalities has been observed in varied amyloid pathologies [31, 32]. Blocking mitochondrial activity and respiration have been reported in case of amyloid proteins such as Aβ and prion protein [33, 34]. Amyloid–mitochondria interactions have been implicated in increased free radicals and reactive oxidative species (ROS) production [35], irregularities of the mitochondrial key enzyme functions [33], mitochondrial calcium release [36], and apoptosis [31]. Amyloid peptides have been also shown to permeabilize mitochondrial membranes [37, 38]. The confocal fluorescence microscopy experiments, utilizing fluorescently-labelled BIM-BH3, confirm cell internalization and mitochondrial uptake of the peptide. Specifically, the fluorescence microscopy images in Fig. 4a demonstrate colocalization of the labelled BIM-BH3 (green) and the mitochondrial dye MitoTracker Orange™ (red), indicating mitochondrial targeting by the peptide.

To assess the effects of BIM-BH3 on mitochondria functionality in living cells we quantified intracellular calcium levels in SH-SY5Y cells incubated with the peptide. Previous studies have shown that amyloid proteins gave rise to elevated levels of intracellular calcium, ascribed to disruption of mitochondria calcium influx [39]. Indeed, the bar diagram in Fig. 4b reveals that intracellular calcium concentrations increased in correlation with BIM-BH3 concentrations. Importantly, treatment of the cells with BIM-BH3 (142–167) did not affect intracellular calcium levels, suggesting that this variant did not disrupt mitochondria functions.

While intracellular calcium levels lead to mitochondrial dysfunction and later to apoptosis [40], an important question one needs to address concerns the effect of BIM-BH3-mediated mitochondrial damage. Figure 4c presents analysis of mitochondrial membrane potential, a common assay for mitochondrial activity. In the experiments, mitochondrial membrane potential depolarization in SH-SY5Y cells was monitored through staining with tetramethylrhodamine ethyl ester (TMRE) [41]. The bar diagram in Fig. 4c indicates that upon addition of 50 μM BIM-BH3, the mitochondrial membrane potential was significantly reduced compared to the untreated control (SH-SY5Y cells without peptide addition). This result is consistent with the flow cytometry experiments in Fig. 3c, showing the apoptotic effect induced by the peptide. Notably, Fig. 4c shows that both the filtered sample of BIM-BH3, and BIM-BH3 (142–167) (50 μM), and did not alter the mitochondrial membrane potential, furnishing additional evidence that the BIM-BH3 fibrils constitute the mitochondrial disruptive species.

To further evaluate the cellular effect of BIM-BH3, we tested its effect of mitochondrial reactive oxygen species (ROS) production as measured using MitoSOX Red™, a mitochondrial superoxide indicator [42]. As shown in Fig. 4d, exposure of SH-SY5Y cells to BIM-BH3 dramatically increased mitochondrial ROS levels. In contrast, the longer peptide domain BIM-BH3 (142–167) had no effect on mitochondrial ROS levels, even at, the highest concentration examined of 50 μM.

Figure 4e illuminates the effects of BIM-BH3 and BIM-BH3 (142–167) upon the activity of the complex IV enzyme-cytochrome c oxidase (COX), which plays a crucial

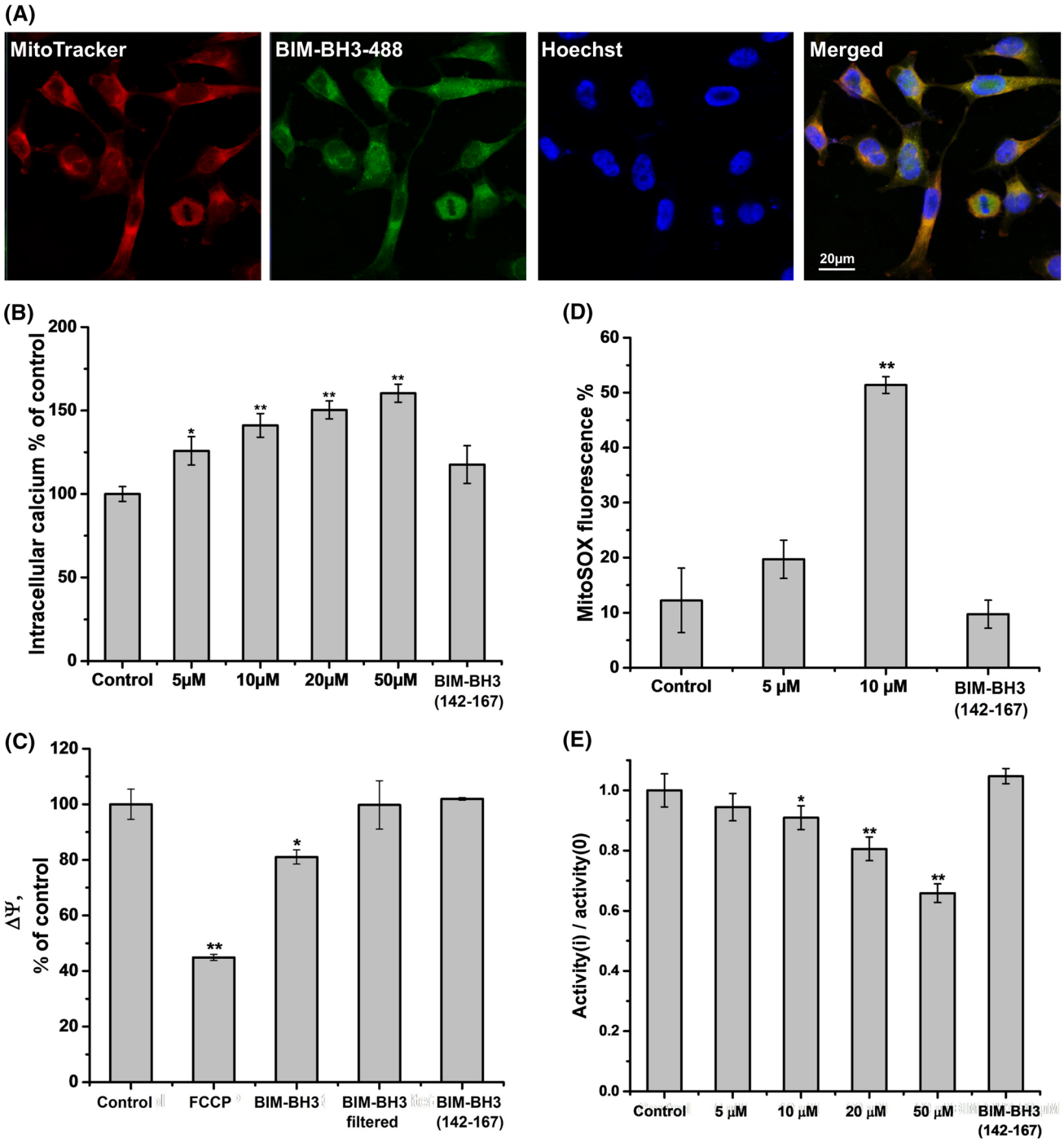

role in mitochondrial functions [43]. Numerous studies have shown that COX activity is reduced in the presence of mitochondria-disrupting substances, including amyloidogenic peptides [44, 45]. In the experiments presented in Fig. 4e, isolated mitochondria from SH-SY5Y cells were ultrasonicated, forming an inside-out oriented submitochondrial particles (SMPs) in which the inner-mitochondrial membrane is exposed to the medium [46]. Subsequently, COX activity was evaluated in the SMP solution by measuring the absorbance (in 550 nm) of a ferrocytochrome c substrate solution. The bar diagram in Fig. 4e demonstrates that COX activity in the isolated SMPs was inversely proportional to BIM-BH3 concentrations, significantly blocked when 50 μM BIM-BH3 was added to the SMPs. In contrast, BIM-BH3 (142–167) did not reduce COX activity, echoing the lack of cell toxicity (Fig. 3), and low disruption of mitochondrial membrane potential (Fig. 4b) recorded for this peptide.

◂**Fig. 4** Disruption of mitochondrial functionality by BIM-BH3. **a** Confocal microscopy analysis of 10 μM BIM-BH3-488 in SH-SY5Y cells. DAPI was used to stain the nuclei and MitoTracker Orange™ was employed to stain mitochondria. Colocalization of BIM-BH3 with the mitochondria is assessed by overlapping of red (mitochondria) and green (BIM-BH3) fluorescence in the merged image. Scale bar corresponds to 10 μm. **b** BIM-BH3-mediated elevation in intracellular calcium levels in SH-SY5Y cells. The cells were incubated with the tested peptides, BIM-BH3 (50–5 μM) or BIM-BH3 (142–167) (50 μM), followed by determination of calcium levels using a direct calcium assay (Fluo-4 direct assay kit). **c** Mitochondrial membrane potential depolarization affected by BIM-BH3 in SH-SY5Y cells. Carbonyl cyanide-*p*-trifluoromethoxy phenylhydrazone (FCCP) served as a control for depolarization of the mitochondrial membrane potential. *Y* axis represents the mitochondrial membrane potential ($\Delta\Psi_m$). **d** Mitochondrial reactive oxidative species (ROS) levels were assessed using MitSOX red and flow cytometry. **e** Cytochrome *c* oxidase (COX) activity measured using submitochondrial particles (SMPs) extracted from SH-SY5Y cells. Values in the *Y* axis represent the COX activity ratio in which *Activity(i)* is the COX activity in SMPs mixed with the tested peptides, BIM-BH3 (50–5 μM) or BIM-BH3 (142–167) (50 μM), and *Activity(0)* is the control (COX activity in SMPs without peptides added). Results are presented as mean ± SEM of three replicates. $*p < 0.05$ and $**p < 0.001$ are compared to control of each experiment

The functional assays in Fig. 4 attest to significant disruption of mitochondrial membrane functionalities by BIM-BH3. Accordingly, we further examined the effect of the peptide upon the mitochondrial membrane organization and functionality which is the main cellular compartment hosting BIM-BH3 peptides (Fig. 5). Figure 5 presents electron spin resonance (ESR) analysis of SMPs prepared from SH-SY5Y cells, doped with the radical probes *N*-tempoyl palmitamide (N-TEMPO) or 10-doxyl nonadecane, following incubation with the BIM-BH3 or BIM-BH3 (142–167). N-TEMPO is localized at the surface of the bilayer [47], while the doxyl radical, linked to carbon in position 10 of the acyl chain, constitutes a sensitive probe of the hydrophobic core of lipid bilayers [48]. The bar diagram in Fig. 5 displays the rotation correlation time ratio ($\frac{\tau_{c(i)}}{\tau_{c(0)}}$) calculated from the ESR spectra (shown in Fig. 6, SI), in which $\tau_{c(i)}$ represents the rotation correlation time of the spin probe measured in vesicles incubated with the peptides, and $\tau_{c(0)}$ corresponds to the correlation time recorded in the control vesicles, prior to peptide addition.

The ESR data in Fig. 5 reveal that BIM-BH3 fibrils exhibited significant interactions with the SMPs, affecting the dynamical features of the embedded spin probes. In the SMPs system containing N-TEMPO, addition of BIM-BH3 fibrils resulted in a concentration-dependent decrease of the rotation correlation time, reflecting a more fluid character of the bilayer. This finding, indicating that the fibrils were primarily localized at the SMPs surface, exhibiting lesser penetration into the bilayer. Importantly, ESR data of bilayer vesicles mimicking the mitochondrial membrane [prepared from dioleylphosphatidylcholine (DOPC) and cardiolipin (CL)], featured similar membrane effects of BIM-BH3 (Fig. 7, SI). This result likely corresponds to the high energy barrier for insertion of the bulky BIM-BH3 fibrils into the bilayer.

Enhanced bilayer fluidity has been previously associated with membrane disruption and cytotoxicity of amyloidogenic peptides [49, 50]. Accordingly, the ESR data in Fig. 5 furnish a possible mechanistic insight linking the apoptotic effects (Fig. 3) and disruption of mitochondrial functions (Fig. 4) to membrane interactions and bilayer reorganization induced by BIM-BH3. Importantly, however, the prominence of BIM-BH3 fibrils in membrane interactions is noteworthy, since in the large majority of amyloid protein systems studied, peptide–membrane interactions (and concomitant toxic effects) have been traced to pre-fibril, oligomeric or monomer assemblies [51–53].

In contrast to the pronounced bilayer effects induced by BIM-BH3, the ESR experiments in Fig. 5 demonstrate that the non-fibril-forming BIM-BH3 (142–167) variant did not affect the rotation correlation times of neither N-TEMPO nor 10-doxyl nonadecane embedded within the SMPs. These results echo the data shown in Figs. 3 and 4, likely accounting for the lack of disruptive cellular effects induced by BIM-BH3 (142–167). Indeed, several studies have indicated that when the BH3 (142–167) variant is bound to its cognate receptor targets, it adopted a α-helical secondary structure [9]. This structural feature stands in contrast to the β-sheet, fibrillar structure of BIM-BH3, linked to the toxic effects of this core protein domain.

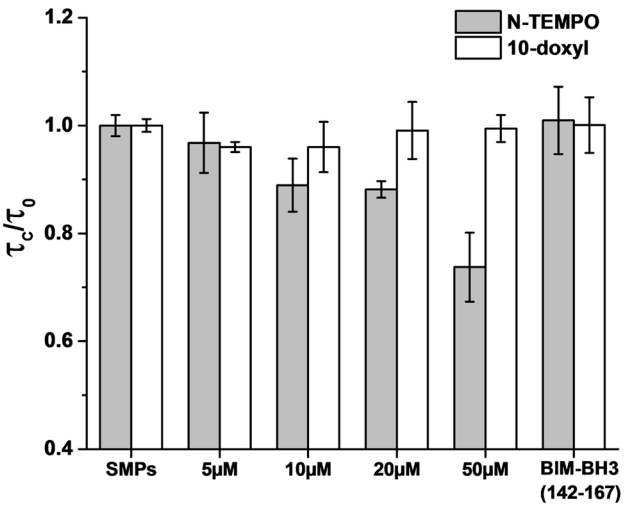

Fig. 5 Effects of the pro-apoptotic domains on the fluidity of mitochondrial membranes. Rotation correlation times τ_c extracted from electron spin resonance (ESR) spectra of TEMPO and 10-doxyl spin probes, respectively, incubated with submitochondrial particles (SMPs) extracted from SH-SY5Y cells. The rotation correlation times were measured following addition of different BIM-BH3 concentrations (50–5 μM), or 50 μM BIM-BH3 (142–167), to the SMPs. Results are presented as mean ± SEM of three replicates

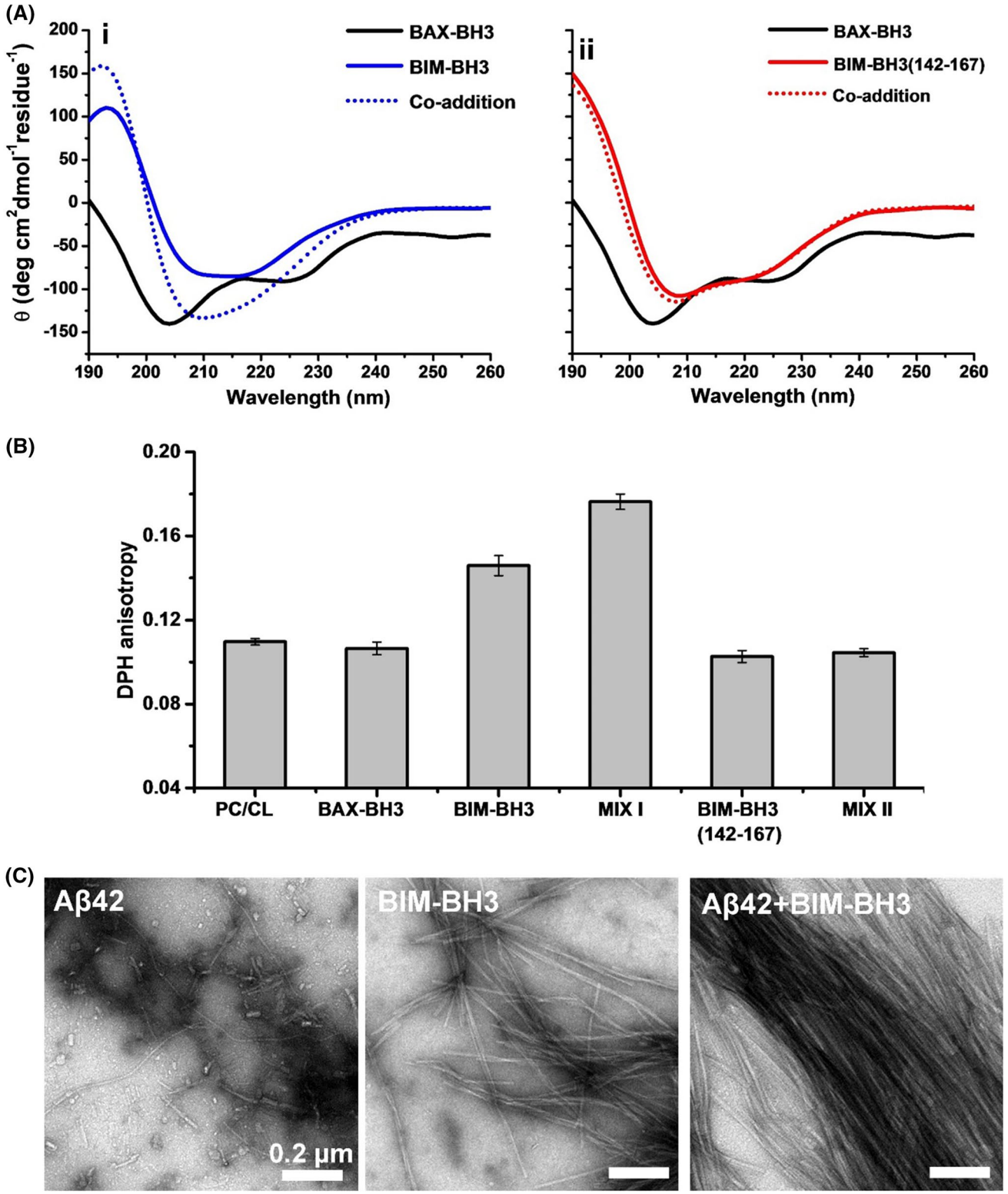

Fig. 6 BIM-BH3 interactions with other proteins. **a** Interactions of BAX-BH3 domain (10 μM) with BIM-BH3 (50 μM) (i) or BIM-BH3 (142–167) (50 μM) (ii). BAX-BH3 alone (black spectra); BIM-BH3 (solid blue); BIM-BH3 + BAX-BH3 (blue dots). BIM-BH3 (142–167) (solid red); BIM-BH3 + BAX-BH3 (red dots). **b** Interactions of BAX-BH3 domain with BIM-BH3 (MIX I) or BIM-BH3 (142–167) (MIX II) with membrane vesicles. Effects of the peptides on bilayer dynamics probed using fluorescence anisotropy measurements. Shown are the fluorescence anisotropy values of DPH embedded in DOPC/cardiolipin vesicles (0.96:0.04 mol ratio). **c** Co-fibrillation of BIM-BH3 and Aβ42. TEM images recorded from solutions of 10 μM Aβ42 alone, 20 μM BIM-BH3 alone, and mixture of Aβ42 (10 μM) and BIM-BH3 (20 μM). Scale bars correspond to 0.2 μm

The remarkable fibrillation of BIM-BH3 raises intriguing questions as to the biological significance of this phenomenon. Accordingly, we investigated the interactions of BIM-BH3 with the BH3 domain of BAX protein (BAX-BH3), one of the important protein targets of BIM-BH3 for triggering apoptosis [8, 24] (Fig. 6a). Indeed, the CD data in Fig. 6a, i reveal significant mutual conformational effects upon co-incubating BIM-BH3 and BAX-BH3. Specifically, BAX-BH3 alone features double minima at 206 and 225 nm [54, 55], while BIM-BH3 in aqueous solution adopted a β-sheet conformation (Fig. 6a, i). Notably, when BIM-BH3 and BAX-BH3 were co-incubated, acceleration of β-sheet assembly was apparent (Fig. 6a, i blue dotted spectrum). In contrast, insignificant conformational change was observed when BAX-BH3 was co-incubated with the non-fibrillar, helical BIM-BH3 (142–167) peptide (Fig. 6a, ii). In that peptide mixture, the helical conformation of BIM-BH3 (142–167) was retained (Fig. 6a, ii, dotted red spectrum). Previous studies indeed reported weak binding and low affinity exist between BIM-BH3 (142–167) and BAX-BH3 [56].

To further probe the interactions between BIM-BH3 and BAX-BH3, we studied the effect of BAX-BH3 upon membrane interactions of the BIM-BH3 fibrils, as the fibrils were shown to significantly affect bilayer dynamics (e.g., Fig. 5). Figure 6b depicts the fluorescence anisotropy values of the fluorescent dye diphenylhexatriene (DPH) embedded within DOPC/CL bilayer vesicles, mimicking the mitochondrial membrane. DPH has been widely employed as a sensitive probe for the effect of membrane-active molecules upon bilayer fluidity and lipid dynamics [57, 58].

The bar diagram in Fig. 6b shows that addition of BIM-BH3 fibrils gave rise to higher fluorescence anisotropy—0.153—of the bilayer-embedded DPH compared to the control vesicles (fluorescence anisotropy of 0.11). This increase in anisotropy likely reflects insertion of the fibrils into the bilayer and its concomitant hardening [58, 59]. BAX-BH3, on the other hand, did not induce an experimentally significant change in bilayer fluidity (Fig. 6b). However, co-incubation of BIM-BH3 and BAX-BH3 affected significantly higher fluorescence anisotropy of DPH (0.18); this dramatic synergistic effect likely accounts to interactions between BIM-BH3 and BAX-BH3, and corroborates the CD results in Fig. 6a. The fluorescence anisotropy experiments further show that neither BIM-BH3 (147–162) alone, nor BIM-BH3 (147–162)/BAX-BH3 mixture, had significant effects upon bilayer fluidity, echoing the CD analysis in Fig. 6a pointing to the lack of interactions between BIM-BH3 (147–162) and BAX-BH3.

A recent report indicated that BIM-BH3 exhibits pronounced effects upon the aggregation properties and cytotoxicity of amyloid-β-42 (Aβ42), the primary constituent of amyloid plaques in neuronal cells inflicted with Alzheimer's disease [59]. Indeed, several studies have identified colocalization of Aβ42 and Bim protein in mitochondrial environments [60, 61]. To test whether interactions occur between BIM-BH3 and Aβ42 we incubated the two peptides together for a few hours and examined the mixture by TEM (Fig. 6). The microscopy results were dramatic, as the BIM-BH3/Aβ42 mixture yielded extensive fibrillation, giving rise to condensed aligned fibrils, which were significantly more ubiquitous than samples of the two peptides separately (TEM images in Fig. 6). The synergistic fibrillation effect suggests a "cross-talk" between BIM-BH3 and Aβ42, similar to phenomena reported for Aβ42 with varied amyloidogenic proteins [62, 63]. The TEM data in Fig. 6 might be physiologically significant, since several studies have identified Aβ42 aggregates in the mitochondria [60, 64].

Conclusions

This study demonstrates that BIM-BH3, the major pro-apoptotic domain of the apoptosis-regulating protein BIM, assembles into amyloid fibrils. The experimental data reveal that BIM-BH3 fibrils, rather than monomeric or oligomeric peptide species, exhibited significant apoptotic activity and disrupted mitochondrial functions. In contrast, the BIM-BH3 (142–167) peptide, 4-residue longer than the core BIM-BH3 domain which widely employed in previous studies and posited as the sequence representing the pro-apoptotic domain in BIM, did not form fibrils, nor exhibited cytotoxicity.

The pronounced difference in structural properties and aggregation profiles between BIM-BH3 and BIM-BH3 (147–162) is significant, as it may point to distinct biological effects of the core BIM-BH3 motif. Furthermore, the interactions and synergistic effects apparent when BIM-BH3 was co-incubated with BAX-BH3, its physiological protein target, may attest to physiological significance of the BIM-BH3 fibrils. Furthermore, the extensive co-fibrillation of BIM-BH3 and Aβ42 may hint at contribution of BIM-BH3 to the cytotoxicity and extensive neuronal cell death, the hallmark of Alzheimer's disease.

Author contributions All authors have given approval to the final version of the manuscript.

Compliance with ethical standards

Conflict of interest The authors declare no competing financial interest.

References

1. Hengartner MO (2000) The biochemistry of apoptosis. Nature 407(6805):770–776
2. O'Brien MA, Kirby R (2008) Apoptosis: a review of pro-apoptotic and anti-apoptotic pathways and dysregulation in disease. J Vet Emerg Crit Care 18(6):572–585
3. Gross A, McDonnell JM, Korsmeyer SJ (1999) BCL-2 family members and the mitochondria in apoptosis. Genes Dev 13(15):1899–1911
4. Kvansakul M, Hinds MG (2015) The Bcl-2 family: structures, interactions and targets for drug discovery. Apoptosis 20(2):136–150
5. Lomonosova E, Chinnadurai G (2008) BH3-only proteins in apoptosis and beyond: an overview. Oncogene 27(1):S2–S19
6. Czabotar PE, Lessene G, Strasser A, Adams JM (2014) Control of apoptosis by the BCL-2 protein family: implications for physiology and therapy. Nat Rev Mol Cell Biol 15(1):49–63
7. Kuwana T, Bouchier-Hayes L, Chipuk JE, Bonzon C, Sullivan BA, Green DR, Newmeyer DD (2005) BH3 domains of BH3-only proteins differentially regulate Bax-mediated mitochondrial membrane permeabilization both directly and indirectly. Mol Cell 17(4):525–535
8. Czabotar P, Colman P, Huang D (2009) Bax activation by Bim? Cell Death Differ 16(9):1187–1191
9. Hinds M, Smits C, Fredericks-Short R, Risk J, Bailey M, Huang D, Day C (2007) Bim, Bad and Bmf: intrinsically unstructured BH3-only proteins that undergo a localized conformational change upon binding to prosurvival Bcl-2 targets. Cell Death Differ 14(1):128–136
10. Delgado-Soler L, Pinto M, Tanaka-Gil K, Rubio-Martinez J (2012) Molecular determinants of Bim (BH3) peptide binding to pro-survival proteins. J Chem Inf Model 52(8):2107–2118
11. Biswas SC, Shi Y, Vonsattel J-PG, Leung CL, Troy CM, Greene LA (2007) Bim is elevated in Alzheimer's disease neurons and is required for β-amyloid-induced neuronal apoptosis. J Neurosci 27(4):893–900
12. Perier C, Bové J, Wu D-C, Dehay B, Choi D-K, Jackson-Lewis V, Rathke-Hartlieb S, Bouillet P, Strasser A, Schulz JB (2007) Two molecular pathways initiate mitochondria-dependent dopaminergic neurodegeneration in experimental Parkinson's disease. Proc Natl Acad Sci 104(19):8161–8166
13. Leon R, Bhagavatula N, Ulukpo O, McCollum M, Wei J (2010) BimEL as a possible molecular link between proteasome dysfunction and cell death induced by mutant huntingtin. Eur J Neurosci 31(11):1915–1925
14. Sanphui P, Biswas S (2013) FoxO3a is activated and executes neuron death via Bim in response to β-amyloid. Cell Death Dis 4(5):e625–e625
15. Engidawork E, Gulesserian T, Seidl R, Cairns N, Lubec G (2001) Expression of apoptosis related proteins in brains of patients with Alzheimer's disease. Neurosci Lett 303(2):79–82
16. Sionov RV, Vlahopoulos SA, Granot Z (2015) Regulation of Bim in health and disease. Oncotarget 6(27):23058
17. Finder VH, Glockshuber R (2007) Amyloid-β aggregation. Neurodegener Dis 4(1):13–27
18. Pillay K, Govender P (2013) Amylin uncovered: a review on the polypeptide responsible for type II diabetes. BioMed Res Int 2013:826706 https://doi.org/10.1155/2013/826706
19. Bates G (2003) Huntingtin aggregation and toxicity in Huntington's disease. Lancet 361(9369):1642–1644
20. Chiti F, Dobson CM (2006) Protein misfolding, functional amyloid, and human disease. Annu Rev Biochem 75:333–366
21. Fowler DM, Koulov AV, Alory-Jost C, Marks MS, Balch WE, Kelly JW (2005) Functional amyloid formation within mammalian tissue. PLoS Biol 4(1):e6
22. Biancalana M, Koide S (2010) Molecular mechanism of Thioflavin-T binding to amyloid fibrils. Biochim Biophys Acta (BBA)-Proteins Proteom 1804(7):1405–1412
23. Lopes AR, Kellam P, Das A, Dunn C, Kwan A, Turner J, Peppa D, Gilson RJ, Gehring A, Bertoletti A (2008) Bim-mediated deletion of antigen-specific CD8 + T cells in patients unable to control HBV infection. J Clin Investig 118(5):1835–1845
24. Robin A, Kumar KK, Westphal D, Wardak A, Thompson G, Dewson G, Colman P, Czabotar P (2015) Crystal structure of Bax bound to the BH3 peptide of Bim identifies important contacts for interaction. Cell Death Dis 6(7):e1809–e1809
25. Czabotar PE, Westphal D, Dewson G, Ma S, Hockings C, Fairlie WD, Lee EF, Yao S, Robin AY, Smith BJ (2013) Bax crystal structures reveal how BH3 domains activate Bax and nucleate its oligomerization to induce apoptosis. Cell 152(3):519–531
26. Stefani M (2010) Biochemical and biophysical features of both oligomer/fibril and cell membrane in amyloid cytotoxicity. FEBS J 277(22):4602–4613
27. Haass C, Selkoe DJ (2007) Soluble protein oligomers in neurodegeneration: lessons from the Alzheimer's amyloid β-peptide. Nat Rev Mol Cell Biol 8(2):101–112
28. Dobson CM (2001) The structural basis of protein folding and its links with human disease. Philos Trans R Soc Lond B Biol Sci 356(1406):133–145
29. Yoshiike Y, Akagi T, Takashima A (2007) Surface structure of amyloid-β fibrils contributes to cytotoxicity. Biochemistry 46(34):9805–9812
30. Oren O, Banerjee V, Taube R, Papo N (2018) An Aβ42 variant that inhibits intra-and extracellular amyloid aggregation and enhances cell viability. Biochem J 475(19):3087–3103
31. Cha M-Y, Han S-H, Son SM, Hong H-S, Choi Y-J, Byun J, Mook-Jung I (2012) Mitochondria-specific accumulation of amyloid β induces mitochondrial dysfunction leading to apoptotic cell death. PloS One 7(4):e34929
32. Lin MT, Beal MF (2006) Mitochondrial dysfunction and oxidative stress in neurodegenerative diseases. Nature 443(7113):787–795
33. Casley C, Canevari L, Land J, Clark J, Sharpe M (2002) β-Amyloid inhibits integrated mitochondrial respiration and key enzyme activities. J Neurochem 80(1):91–100
34. O'Donovan CN, Tobin D, Cotter TG (2001) Prion protein fragment PrP-(106–126) induces apoptosis via mitochondrial disruption in human neuronal SH-SY5Y cells. J Biol Chem 276(47):43516–43523
35. Reddy PH (2009) Amyloid beta, mitochondrial structural and functional dynamics in Alzheimer's disease. Exp Neurol 218(2):286–292
36. Ferreiro E, Oliveira CR, Pereira CM (2008) The release of calcium from the endoplasmic reticulum induced by amyloid-beta and prion peptides activates the mitochondrial apoptotic pathway. Neurobiol Dis 30(3):331–342
37. Kagan BL, Thundimadathil J (2010) Amyloid peptide pores and the beta sheet conformation. In: Proteins membrane binding and pore formation. Springer, New York, pp 150–167
38. Meratan AA, Ghasemi A, Nemat-Gorgani M (2011) Membrane integrity and amyloid cytotoxicity: a model study involving mitochondria and lysozyme fibrillation products. J Mol Biol 409(5):826–838
39. Oren O, Ben Zichri S, Taube R, Jelinek R, Papo N (2020) Aβ42 double mutant inhibits Aβ42-induced plasma and mitochondrial membrane disruption in artificial membranes, isolated organs, and intact cells. ACS Chem Neurosci 11(7):1027–1037

40. Kruman I, Guo Q, Mattson MP (1998) Calcium and reactive oxygen species mediate staurosporine-induced mitochondrial dysfunction and apoptosis in PC12 cells. J Neurosci Res 51(3):293–308
41. Ly JD, Grubb DR, Lawen A (2003) The mitochondrial membrane potential ($\Delta\psi$ m) in apoptosis; an update. Apoptosis 8(2):115–128
42. Ben-Hail D, Begas-Shvartz R, Shalev M, Shteinfer-Kuzmine A, Gruzman A, Reina S, De Pinto V, Shoshan-Barmatz V (2016) Novel compounds targeting the mitochondrial protein VDAC1 inhibit apoptosis and protect against mitochondrial dysfunction. J Biol Chem 291(48):24986–25003
43. Capaldi RA (1990) Structure and function of cytochrome *c* oxidase. Annu Rev Biochem 59(1):569–596
44. Fukui H, Diaz F, Garcia S, Moraes CT (2007) Cytochrome c oxidase deficiency in neurons decreases both oxidative stress and amyloid formation in a mouse model of Alzheimer's disease. Proc Natl Acad Sci 104(35):14163–14168
45. Hong WK, Han EH, Kim DG, Ahn JY, Park JS, Han BG (2007) Amyloid-β-peptide reduces the expression level of mitochondrial cytochrome oxidase subunits. Neurochem Res 32(9):1483–1488
46. Lee CP (1979) [12] Tightly coupled beef heart submitochondrial particles. In: Methods in enzymology, vol 55. Academic Press, pp 105–112
47. Lally CCM, Bauer B, Selent J, Sommer ME (2017) C-edge loops of arrestin function as a membrane anchor. Nat Communications 8(1):1–12
48. Vogel A, Scheidt HA, Huster D (2003) The distribution of lipid attached spin probes in bilayers: application to membrane protein topology. Biophys J 85(3):1691–1701
49. Avdulov NA, Chochina SV, Igbavboa U, O'Hare EO, Schroeder F, Cleary JP, Wood WG (1997) Amyloid β-peptides increase annular and bulk fluidity and induce lipid peroxidation in brain synaptic plasma membranes. J Neurochem 68(5):2086–2091
50. Chochina S, Avdulov N, Igbavboa U, Cleary J, O'Hare E, Wood W (2001) Amyloid β-peptide1-40 increases neuronal membrane fluidity: role of cholesterol and brain region. J Lipid Res 42(8):1292–1297
51. Malishev R, Shaham-Niv S, Nandi S, Kolusheva S, Gazit E, Jelinek R (2017) Bacoside-A, an Indian traditional-medicine substance, inhibits β-amyloid cytotoxicity, fibrillation, and membrane interactions. ACS Chem Neurosci 8(4):884–891
52. Williams TL, Serpell LC (2011) Membrane and surface interactions of Alzheimer's Aβ peptide–insights into the mechanism of cytotoxicity. FEBS J 278(20):3905–3917
53. Lee SJC, Nam E, Lee HJ, Savelieff MG, Lim MH (2017) Towards an understanding of amyloid-β oligomers: characterization, toxicity mechanisms, and inhibitors. Chem Soc Rev 46(2):310–323
54. Harris MM, Coon Z, Alqaeisoom N, Swords B, Holub JM (2016) Targeting anti-apoptotic Bcl2 proteins with scyllatoxin-based BH3 domain mimetics. Org Biomol Chem 14(2):440–446
55. Wang D, Liao W, Arora PS (2005) Enhanced metabolic stability and protein-binding properties of artificial α helices derived from a hydrogen-bond surrogate: application to Bcl-xL. Angew Chem Int Ed 44(40):6525–6529
56. Willis SN, Fletcher JI, Kaufmann T, van Delft MF, Chen L, Czabotar PE, Ierino H, Lee EF, Fairlie WD, Bouillet P (2007) Apoptosis initiated when BH3 ligands engage multiple Bcl-2 homologs, not Bax or Bak. Science 315(5813):856–859
57. Suzuki M (1848) Miura T (2015) Effect of amyloid β-peptide on the fluidity of phosphatidylcholine membranes: uses and limitations of diphenylhexatriene fluorescence anisotropy. Biochim Biophys Acta (BBA) Biomembr 1848(3):753–759
58. Malishev R, Arad E, Bhunia SK, Shaham-Niv S, Kolusheva S, Gazit E, Jelinek R (2018) Chiral modulation of amyloid beta fibrillation and cytotoxicity by enantiomeric carbon dots. Chem Commun 54(56):7762–7765
59. Malishev R, Nandi S, Śmiłowicz D, Bakavayev S, Engel S, Bujanover N, Gazit R, Metzler-Nolte N, Jelinek R (2019) Interactions between BIM protein and beta-amyloid may reveal a crucial missing link between Alzheimer's disease and neuronal cell death. ACS Chem Neurosci 10(8):3555–3564
60. Petersen CAH, Alikhani N, Behbahani H, Wiehager B, Pavlov PF, Alafuzoff I, Leinonen V, Ito A, Winblad B, Glaser E (2008) The amyloid β-peptide is imported into mitochondria via the TOM import machinery and localized to mitochondrial cristae. Proc Natl Acad Sci 105(35):13145–13150
61. Yin K, Lee J-M, Chen S, Xu J, Hsu CY (2002) Amyloid-β induces Smac release via AP-1/Bim activation in cerebral endothelial cells. J Neurosci 22(22):9764–9770
62. Seeliger J, Evers F, Jeworrek C, Kapoor S, Weise K, Andreetto E, Tolan M, Kapurniotu A, Winter R (2012) Cross-amyloid interaction of Aβ and IAPP at lipid membranes. Angew Chem Int Ed 51(3):679–683
63. Luo J, Wärmländer SK, Gräslund A, Abrahams JP (2016) Cross-interactions between the Alzheimer disease amyloid-β peptide and other amyloid proteins: a further aspect of the amyloid cascade hypothesis. J Biol Chem 291(32):16485–16493
64. Wang X, Su B, Perry G, Smith MA, Zhu X (2007) Insights into amyloid-β-induced mitochondrial dysfunction in Alzheimer disease. Free Radic Biol Med 43(12):1569–1573